DR MARTIN LOHR (Orcid ID : 0000-0002-4335-9887)

Article type : Original Article

A functional zeaxanthin epoxidase from red algae shedding light on the evolution of light-harvesting carotenoids and the xanthophyll cycle in photosynthetic eukaryotes

Oliver Dautermann, Martin Lohr

Johannes Gutenberg-Universität, Institut für Molekulare Physiologie, Pflanzenbiochemie, Johannes-von-Müller-Weg 6, 55128 Mainz, Germany

Corresponding author:
Dr. Martin Lohr
Johannes Gutenberg-Universität
Institut für Molekulare Physiologie, Pflanzenbiochemie
Johannes-von-Müller-Weg 6
55128 Mainz, Germany
Tel.: +49-6131-3924201; Fax: +49-6131-3923075; E-Mail: Lohr@uni-mainz.de

Running Head: Zeaxanthin epoxidase in red algae

Keywords: zeaxanthin epoxidase, antheraxanthin, carotenoid biosynthesis, Rhodophyta, *Madagascaria erythrocladioides*, chromalveolates, photoprotection, light-harvesting

Summary

The epoxy-xanthophylls antheraxanthin and violaxanthin are key precursors of light-harvesting carotenoids and participate in the photoprotective xanthophyll cycle. Thus, the invention of zeaxanthin epoxidase (ZEP) catalyzing their formation from zeaxanthin has been a fundamental step in the evolution of photosynthetic eukaryotes. ZEP genes have only been found in Viridiplantae and chromalveolate algae with secondary plastids of red algal ancestry, suggesting that ZEP evolved in the Viridiplantae and spread to chromalveolates by lateral gene transfer.

By searching publicly available sequence data from eleven red algae covering all currently recognized red algal classes we identified ZEP candidates in three species. Phylogenetic analyses showed that the red algal ZEP is most closely related to ZEP proteins from photosynthetic chromalveolates possessing secondary plastids of red algal origin. Its enzymatic activity was assessed by HPLC analyses of red algal pigment extracts and by cloning and functional expression of the ZEP gene from *Madagascaria erythrocladioides* in leaves of the ZEP-deficient *aba2* mutant of *Nicotiana plumbaginifolia*. Unlike other ZEP enzymes examined so far, the red algal ZEP introduces only a single epoxy group into zeaxanthin, yielding antheraxanthin instead of violaxanthin. The results indicate that ZEP evolved before the split of Rhodophyta and Viridiplantae and that chromalveolates acquired ZEP from the red algal endosymbiont and not by lateral gene transfer. Moreover, the red algal ZEP enables engineering of transgenic plants incorporating antheraxanthin instead of violaxanthin in their photosynthetic machinery.

Introduction

The initial event in the birth of photosynthetic eukaryotes was the endosymbiotic uptake of an early cyanobacterium by a heterotrophic eukaryote more than 1.5 Ga ago (Yoon *et al.*, 2004; Yang *et al.*, 2016). During stabilization of this endosymbiotic association most of the photosynthesis-related genes were transferred from the endosymbiont to the host genome, ultimately turning the endosymbiotic bacterium into a plastid. As a consequence, in photosynthetic eukaryotes nucleus-encoded plastid proteins are synthesized in the cytosol and retargeted to the plastids by N-terminal transit sequences.

This endosymbiotic event gave rise to the three extant major groups with primary plastids, the glaucophyte algae (Glaucophyta), the red algae (Rhodophyta) and the green algae and land plants (Viridiplantae) (Price *et al.*, 2012; Jackson & Reyes-Prieto, 2014; Li *et al.*, 2014). Several algal groups acquired their plastids secondarily by taking up either a green or a red alga as endosymbiont, followed by transfer of plastid genes to the nucleus of the second host and ultimately the reduction of the primary host to its plastids. Major marine primary producers such as diatoms, haptophytes and dinoflagellates have secondary plastids of red algal origin. The chromalveolate hypothesis states that these algal groups originated from a single secondary endosymbiosis and thus are monophyletic. Although this is a matter of ongoing controversy (Stiller *et al.*, 2014; Cavalier-Smith *et al.*, 2015; Gould *et al.*, 2015), these algal groups collectively will be referred to as chromalveolates throughout.

A comparison of the photosynthetic apparatus of extant cyanobacteria with that of plastids from photosynthetic eukaryotes indicates that Glaucophyta and Rhodophyta retained the tetrapyrrole-based phycobiliproteins as light-harvesting antennae. Their carotenoid pattern is rather simple with β-carotene and zeaxanthin as major components, the latter being replaced by lutein in some groups of red algae (Marquardt & Hanelt, 2004; Schubert *et al.*, 2006; Jeffrey *et al.*, 2011; Takaichi *et al.*, 2016) (**Figure 1**).

In green algae and most chromalveolates, carotenoids have gained increasing importance particularly in light-harvesting, which is reflected in a more complex carotenoid composition. The light-harvesting complexes of land plants and most green algae contain lutein and the epoxy-xanthophylls violaxanthin and 9'-*cis*-neoxanthin (**Figure 1**), the latter also being the precursor of the phytohormone abscisic acid (Nambara & Marion-Poll, 2005). Chromalveolate algae synthesize allenic carotenoids such as fucoxanthin, peridinin or vaucheriaxanthin acyl esters and acetylenic carotenoids like diadinoxanthin and diatoxanthin. Theoretical considerations and experimental evidence (Swift & Milborrow, 1981; Lohr & Wilhelm, 1999; Lohr & Wilhelm, 2001) indicate that violaxanthin is a central intermediate in the formation of the allenic and acetylenic xanthophylls in chromalveolates; rearrangement of one of the 5,6-epoxy groups in violaxanthin to a hydroxy group at C5 enables formation of the C6-C8 allenic group, and dehydration yields the acetylenic group at C7 (**Figure 1**). Moreover, violaxanthin or alternatively the acetylenic epoxy-xanthophyll diadinoxanthin are involved in the photoprotective xanthophyll cycle present in most algal groups (Goss & Lepetit, 2015). Under excess light conditions, these pigments are converted by violaxanthin de-epoxidase (VDE) to zeaxanthin or diatoxanthin, respectively, thereby promoting non-photochemical

quenching of excited chlorophyll molecules in the light-harvesting complexes (Goss & Lepetit, 2015; Ruban, 2016). Thus, the ability to synthesize 5,6-epoxy-xanthophylls has been a major advancement in the evolution of the photosynthetic machineries of algae and ultimately also land plants.

In land plants and green algae, violaxanthin is synthesized from zeaxanthin via the intermediate antheraxanthin by zeaxanthin epoxidase (ZEP) (Marin *et al.*, 1996; Baroli *et al.*, 2003). The nucleus-encoded plastid enzyme is located predominantly at the stromal side of the thylakoid membranes, needs FAD as cofactor and molecular oxygen and NADPH as cosubstrates and is responsible for de-novo formation of violaxanthin and neoxanthin as well as the back reaction of the photoprotective xanthophyll cycle (Siefermann & Yamamoto, 1975; Büch *et al.*, 1995; Schwarz *et al.*, 2015). In line with the presence of epoxy-xanthophylls and xanthophyll cycles in chromalveolate algae, their genomes also have been found to encode putative ZEP proteins (Coesel *et al.*, 2008; Frommolt *et al.*, 2008). Recently, epoxidase activity has been confirmed for ZEP candidates from two chromalveolate algae, the diatom *Phaeodactylum tricornutum* (Eilers *et al.*, 2016) and the eustigmatophyte *Nannochloropsis oceanica* (Leonelli *et al.*, 2016).

Xanthophylls with 5,6-epoxy groups such as antheraxanthin and violaxanthin have not yet been reported from cyanobacteria (Goodwin, 1980; Takaichi & Mochimaru, 2007) and are also absent from glaucophytes and most red algae (Marquardt & Hanelt, 2004; Schubert *et al.*, 2006; Jeffrey *et al.*, 2011; Takaichi *et al.*, 2016). In a number of red algae of the orders Corallinales, Ceramiales and Gracilariales within the class Florideophyceae and of the order Erythropeltidales (class Bangiophyceae), though, antheraxanthin and occasionally small amounts of violaxanthin have been detected (Aihara & Yamamoto, 1968; Brown & Mclachlan, 1982; Bjørnland *et al.*, 1984; Andersson *et al.*, 2006; Schubert *et al.*, 2006; Takaichi *et al.*, 2016). The molecular basis of their ability to synthesize epoxy-xanthophylls, however, is not known (Takaichi *et al.*, 2016), and the occurrence of xanthophyll cycling in red algae is doubtful (Frommolt *et al.*, 2008; Schubert & García-Mendoza, 2008; Esteban *et al.*, 2009).

Based on sequence similarity on the protein level, putative ZEP genes have been reported from several red algae of the order Bangiales. ZEP-related sequences were found in two species of *Porphyra* and in *Pyropia yezoensis* (Yang *et al.*, 2014; Mikami *et al.*, 2016), but HPLC analyses failed to detect epoxy-carotenoids in any of these species (Schubert *et al.*, 2006; Gantt *et al.*, 2010; Yang *et al.*, 2014; Takaichi *et al.*, 2016). Recently, genomic and

transcriptomic sequence data have become available from an increasing number of algae, enabling homology-based searches for candidate genes involved in biochemical pathways with a much broader taxon sampling. This situation enabled us to search for ZEP candidates in additional red algae covering all seven currently recognized classes (Yoon *et al.*, 2006), namely Cyanidiophyceae, Compsopogonophyceae, Porphyridiophyceae, Rhodellophyceae, Stylematophyceae, Bangiophyceae and Florideophycea (**Table S1**).

Here, we show that three antheraxanthin-accumulating red algae contain a gene encoding a protein with close phylogenetic affiliation to ZEP proteins from plants and other algae. Employing a rapid method for functional expression of ZEP candidate genes in a ZEP-deficient tobacco mutant we furthermore demonstrate that the red algal gene encodes a functional ZEP whose substrate specificity differs from that of already characterized ZEP proteins. *In silico* analyses of the previously identified ZEP candidates from Bangiophyceae, on the other hand, suggest that they are probably not involved in plastidic carotenoid metabolism.

Results

Identification of ZEP candidate genes from red algae

The Basic Local Alignment Search Tool (BLAST) was used to search in publicly available sequence data from cyanobacteria, glaucophytes and rhodophytes for genes encoding proteins with high similarity to the ZEP sequence from *Arabidopsis thaliana* (AtZEP). The search included transcriptomic data from two glaucophytes and eleven rhodophytes, genomic data of the glaucophyte *Cyanophora paradoxa* and four red algae (see **Table S1** for details), and all cyanobacterial sequences in the non-redundant protein sequences (nr) database of NCBI. To avoid exclusion of short sequences, no fixed cutoff for E-values was used. Instead, a careful inspection of the BLAST results was performed.

In the first round of searches, we identified partial sequences of ZEP candidates with protein sequence similarities to AtZEP between 60 and 65% from three red algae, namely the two Compsopogonophyceae *Compsopogon coeruleus* and *Madagascaria erythrocladioides,* and *Calliarthron tuberculosum* belonging to the Corallinales. The partial sequences from *C. coeruleus* and *M. erythrocladioides* (two for each species) were linked and extended by additional BLAST searches in the SRA database of NCBI, yielding for *C. coeruleus* an ORF of

1109 bp with incomplete 5'-end (**Data S1)**. For *M. erythrocladioides*, two putative alleles with ORFs of 1404 and 1413 bp were identified that could be amplified from genomic DNA of *M. erythrocladioides* (GenBank accessions MF380407 and MF380408; see also **Data S2**). Both alleles contain a conserved intron of 53 bp, but differ in length by an indel of 9 base pairs close to the 3'-end of their second exon. In addition, they show 13 single-base substitutions, two of which result in amino acid substitutions (R15S and E99D). For *C. tuberculosum*, eight genomic reads were identified in the NCBI-SRA database that could be assembled into two contigs (**Data S3**). One contig containing six reads covered the 5'-end of a putative ZEP gene with a partial ORF of 896 bp including a potential start codon. The other contig comprised of two reads covered the 3'-end with a partial ORF of 416 bp including a stop codon.

Of the best hits from cyanobacteria, several had been annotated as zeaxanthin epoxidases. For our *in silico* analyses, we retrieved cyanobacterial sequences putatively assigned as zeaxanthin epoxidases comprising proteins from eight different species (**Table S2**). We also included the putative ZEP proteins from the three Bangiales *Porphyra purpurea, P. umbilicalis* and *Pyropia yezoensis* (Mikami *et al.*, 2016) after careful reexamination of their N-termini by BLAST searches in the SRA database of NCBI and the genomic scaffolds of *P. yezoensis* (assembly version 1; Nakamura et al., 2013) and correction of the 5'-ends of the ZEP candidate genes from *P. purpurea* and *P. umbilicalis* (**Data S4, S5 and S6**).

Phylogenetic analyses indicated that the red algal ZEP candidates are most closely related to the ZEP proteins from heterokont and haptophyte algae, forming a cluster that is sister to the ZEP from Viridiplantae (**Figure 2a**). In this cluster, enzymatic activity has recently been confirmed for two ZEP candidates from the diatom *Phaeodactylum tricornutum* (Eilers *et al.*, 2016) and the ZEP from *Nannochloropsis oceanica* (Leonelli *et al.*, 2016). The putative ZEP proteins from the three Bangiophyceae and the cyanobacterial proteins annotated as zeaxanthin epoxidases, however, were positioned on long branches well separated from the clusters of ZEP proteins with confirmed epoxidase activity (**Figure 2a**).

Moreover, *in silico* analyses of the amino acid sequences of the ZEP candidates from *M. erythrocladioides* and *C. tuberculosum* predicted the presence of N-terminal signals for targeting of the proteins to plastids (**Figure 2b**). In agreement with this prediction both sequences contained a phenylalanine residue close to the start methionine that is diagnostic for transit peptides from red algae and glaucophytes (Steiner & Löffelhardt, 2005; Patron & Waller, 2007). The ZEP candidates from the three Bangiophyceae, on the other hand, had

significantly shorter N-termini with no resemblance to canonical transit peptides (**Figure 2b**), indicating the lack of plastid targeting signals. This was not due to incomplete N-termini, as no other potential in-frame start codons were present upstream of the predicted coding sequences and two of the three genes contained in-frame stop codons upstream of the start codon (**Data S7**).

The red algal ZEP converts zeaxanthin to antheraxanthin

In line with the identification of a putative ZEP in *C. tuberculosum*, this alga had already been reported to contain epoxy-carotenoids (Schubert *et al.*, 2006). Recently, the presence of antheraxanthin has also been reported for a natural sample of *C. coeruleus* (Takaichi *et al.*, 2016), but no pigment data were available for isolated strains of *C. coeruleus* and for *M. erythrocladioides*. Therefore, we analyzed the pigment content of *M. erythrocladioides*, two strains of *C. coeruleus*, and the closely related species *C. hookeri*, *C. oishii*, *Compsopogonopsis leptoclados* and *Rhodochaete parvula*. As a positive control, we included *Erythrotrichia carnea* reported before to contain antheraxanthin (Bjørnland *et al.*, 1984). HPLC analyses of pigment extracts confirmed the presence of substantial amounts of antheraxanthin in all eight strains of Compsopogonophyceae, while violaxanthin was not detectable or only present in traces (**Table 1** and **Figure 3a**). The identity of antheraxanthin from the red algae was confirmed by comparison of retention times and UV/VIS-absorbance spectra with an antheraxanthin standard, by furanoid rearrangement of the isolated pigment indicating the presence of a single 5,6-epoxy group (**Figure 3b**), and by its enzymatic de-epoxidation to zeaxanthin in an *in vitro* assay using violaxanthin de-epoxidase from *A. thaliana* (**Figure 3c**).

Next, we aimed at investigating the catalytic activity of the protein encoded by a red algal ZEP gene. As our efforts of functional expression of several algal ZEP genes in bacteria had been unsuccessful, we attempted *Agrobacterium*-mediated transient expression of a red algal ZEP gene in tobacco leaves. To avoid interference of the endogenous ZEP, we chose the ZEP-deficient *aba2* mutant of *Nicotiana plumbaginifolia* that had enabled the identification of the first ZEP gene from plants (Marin *et al.*, 1996).

For a proof of concept, we generated a construct containing the ZEP gene from *A. thaliana* (AtZEP) in the binary pPZP200BAR vector (Hajdukiewicz *et al.*, 1994) and used the resulting plasmid pPZPbar-tpAtZEP-AtZEP for *Agrobacterium*-mediated transformation of leaves of

the *N. plumbaginifolia aba2* mutant. HPLC analysis of pigment extracts from untreated leaves and from leaves 4 d after infiltration showed that introduction of the AtZEP gene restored the biosynthesis of the epoxy-carotenoids violaxanthin and neoxanthin in the mutant (**Figure 4a**). In addition, small amounts of lutein epoxide were detectable. The ability of the N-terminal transit sequence of the AtZEP to enable import of other proteins into the tobacco plastids was further demonstrated by fusing a gene fragment encoding the transit peptide comprising 66 amino acids (tp_{AtZEP}) with the gene encoding GFP. Confocal laser scanning microscopy of leaves from *N. plumbaginifolia* transformed with the tp_{AtZEP}-GFP-gene (plasmid pPZPbar-tpAtZEP-GFP) showed green-fluorescing plastids while GFP without the N-terminal transit peptide (plasmid pPZPbar-GFP) remained in the cytosol (**Figure 4b-g**), implying that the transit peptide of AtZEP is generally suitable for targeting foreign proteins into the plastids of *N. plumbaginifolia*.

We then cloned both alleles of the candidate ZEP gene from *M. erythrocladioides* (MeZEP) from nucleotide position 55 of the predicted ORF to the stop codon (GenBank accessions MF152645 and MF543015). The MeZEP genes were placed in frame behind the tp_{AtZEP}-gene fragment in the pPZP200BAR-vector and the resulting constructs (pPZPbar-tp_{AtZEP}-MeZEPa1 and pPZPbar-tp_{AtZEP}-MeZEPa2) used for transformation of the tobacco *aba2* mutant. HPLC-analysis of pigment extracts from mutant leaves 4 d after infiltration (**Figure 4a**) showed a new pronounced peak that was identified as antheraxanthin using the same methods as shown in **Figure 3**, while violaxanthin and neoxanthin were not detectable. The formation of antheraxanthin was accompanied by a corresponding reduction of zeaxanthin in the transformed leaves. The transformants also accumulated minor amounts of lutein epoxide (below 10% of the content of antheraxanthin), as observed before in *aba2* mutants transformed with AtZEP. Both MeZEP alleles resulted in the same pigment phenotype.

Discussion

Although the presence of antheraxanthin in red algae is well established, the molecular details of its biosynthesis in rhodophytes have been unknown. The preferred accumulation of antheraxanthin instead of violaxanthin and the apparent lack of xanthophyll cycling in red algae (Marquardt & Hanelt, 2004; Schubert & García-Mendoza, 2008; Esteban *et al.*, 2009) led to speculations that red algae possess an epoxidase that is unrelated to ZEP from land plants and other algae (Takaichi *et al.*, 2016). Moreover, comparative genomics of carotenoid

biosynthesis genes in algae led us to propose that ZEP may have evolved in early green algae and been transferred to algae with secondary red plastids by lateral gene transfer or a cryptic green endosymbiont (Frommolt *et al.*, 2008; Moustafa *et al.*, 2009).

Identification of a functional ZEP from red algae

Here, we have identified three rhodophyte species encoding a protein closely related to ZEP enzymes with proven catalytic activity from chromalveolate algae with secondary red plastids (**Figure 2a**). For *C. coeruleus*, *M. erythrocladioides* and four closely related species, we established by HPLC the presence of antheraxanthin (**Table 1** and **Figure 3**), while *C. tuberculosum* had already been reported to contain antheraxanthin (Schubert *et al.*, 2006). The configuration of the pigment identified as antheraxanthin in all red algae examined here is probably identical to that of antheraxanthin from land plants, namely (3*S*,5*R*,6*S*,3'*R*). This conclusion is based on the violaxanthin de-epoxidase assay we used **(Figure 3c**), because violaxanthin de-epoxidase from land plants has been shown to be specific for antheraxanthin and to discriminate antheraxanthin B having (3*S*,5*S*,6*R*,3'*R*)-configuration (Yamamoto & Higashi, 1978). For antheraxanthin from *E. carnea*, (3*S*,5*R*,6*S*,3'*R*)-configuration has been established before by NMR spectroscopy (Bjørnland *et al.*, 1984).

The co-occurrence of antheraxanthin and the candidate gene for ZEP in all three rhodophytes already indicated that the product of this gene may catalyze the formation of antheraxanthin in red algae. Expression of the ZEP candidate from *M. erythrocladioides* (MeZEP) in the ZEP-deficient *aba2* mutant of *N. plumbaginifolia* resulted in the accumulation of antheraxanthin but not violaxanthin, strongly supporting the conclusion that the identified ZEP gene is also responsible for antheraxanthin biosynthesis in *M. erythrocladioides*. Further support comes from our *in silico* analyses that predicted the presence of N-terminal transit peptides typical for nucleus-encoded plastid proteins in the ZEP sequences from *M. erythrocladioides* and *C. tuberculosus*. A recent study failed to identify a ZEP candidate in *C. tuberculosus* (Takaichi *et al.*, 2016), but there only the protein models predicted by AUGUSTUS were searched which lacked a ZEP homologue, while we retrieved eight partial ZEP sequences from the NCBI-SRA database (**Data S3**).

The lack of transit peptides and the more distant relationship of the ZEP-like proteins from *Pyropia yezoensis*, *Porphyra purpurea* and *P. umbilicalis* to ZEP proteins with proven catalytic activity (**Figure 2**), together with the absence of epoxy-carotenoids in the three algae (Schubert *et al.*, 2006; Gantt *et al.*, 2010; Yang *et al.*, 2014; Takaichi *et al.*, 2016) argue

against their previous assignment as zeaxanthin epoxidases. Based on the phylogenetic tree in **Figure 2** and the absence of epoxy-carotenoids in *Calothrix* sp. 336/3 (Kosourov *et al.*, 2016) and cyanobacteria in general (Goodwin, 1980; Takaichi & Mochimaru, 2007), the cyanobacterial sequences that have been annotated as zeaxanthin epoxidases probably also serve other functions than carotenoid biosynthesis. Like ZEP, these proteins belong to the extended family of class A flavoprotein monoxygenases that have aromatic compounds with an activating hydroxyl or amino group as typical substrates (van Berkel *et al.*, 2006), suggesting a variety of potential substrates other than carotenoids.

It remains to be explored which amino acid residues determine the atypical substrate specificity of the red algal ZEP. The ZEP protein from *M. erythrocladioides* shows only 46% identity and 67% similarity to the most closely related ZEP with proven catalytic function from the eustigmatophyte *Nannochloropsis oceanica* (**Figure 2a**). Such a large variance between sequences impedes identification of the potentially small differences critical for altered substrate specificity by sequence comparisons, even when highly variable regions are excluded from the analyses. To narrow down possibilities to a few potentially important regions, either more distantly related ZEP proteins that exclude antheraxanthin as substrate, or a closely related red algal ZEP converting at least some antheraxanthin further to violaxanthin would need to be identified. The latter type of ZEP may be present in *Delesseria lancifolia* and some species of the genus *Gracilaria* as indicated by their pigment phenotypes (**Table 1**).

Evidence that ZEP evolved before the split of Rhodophyta and Viridiplanta

Antheraxanthin has been detected in all Compsopogonophyceae investigated so far and in various species of the Ceramiales, Gracilariales and the subfamily Corallinoideae within Corallinales (**Table 1)**, while the majority of red algal taxa appear to lack the ability to synthesize epoxy-carotenoids (Schubert *et al.*, 2006; Takaichi *et al.*, 2016). Therefore, if the presence of a ZEP gene is the ancestral state in red algae, multiple independent losses of ZEP must have occurred among rhodophytes. Nevertheless, the close phylogenetic affiliation of the ZEP proteins from the two Compsopogonophyceae and from *Calliarthron* of the Florideophyceae (**Figure 2a**) – two classes estimated to be separated since about 1.2 Ga (Yang *et al.*, 2016) – indicates that their genes derived from the same ancestral ZEP gene by speciation and are not the result of more recent independent horizontal gene transfers. This probably extends to the yet unidentified ZEP genes from algae of other orders of the

Florideophyceae, as all these algae accumulate antheraxanthin as the main epoxycarotenoid, suggesting that their ZEP proteins share the same atypical substrate specificity due to a common ancestry. The lack of ZEP genes in cyanobacteria and glaucophytes and the close affiliation of ZEP from red and green algae (**Figure 2a**) suggest that ZEP evolved in the common ancestor of red and green algae after separation of the glaucophytes. Furthermore, the close phylogenetic affiliation of the red algal ZEP with ZEP proteins from chromalveolate algae (**Figure 2a**) favors the hypothesis that chromalveolates acquired their ZEP genes from the red algal endosymbiont and not from an ancient green alga as proposed earlier (Frommolt *et al.*, 2008).

Potential roles of antheraxanthin in the photosynthetic apparatus of red algae and green plants

The biological significance of antheraxanthin in red algae and its localization in the photosynthetic apparatus are still unclear. In natural samples of red algae the ratio of antheraxanthin to other carotenoids varied with seasons (Esteban *et al.*, 2009) and depth (Schubert & García-Mendoza, 2008), indicating a positive correlation to growth light intensity. These observations suggest that antheraxanthin in red algae may also be involved in photoprotection, but experimental support for this hypothesis is still lacking. On the other hand, the discovery of a ZEP catalyzing the epoxidation of only one ionone ring in zeaxanthin offers the possibility of engineering transgenic land plants or green algae that contain antheraxanthin instead of violaxanthin in their photosynthetic machinery. Mutants of *A. thaliana* and the green alga *Chlamydomonas reinhardtii* with altered carotenoid composition such as deficiency in lutein or epoxy-carotenoids have been instrumental for assessing the contribution of different carotenoids to light-harvesting, photoprotection or stabilization of photosynthetic pigment-protein complexes (Pogson *et al.*, 1996; Niyogi *et al.*, 1997b; Niyogi *et al.*, 1998; Pogson *et al.*, 1998; Lokstein *et al.*, 2002). Moreover, the characterization of these mutants revealed a remarkable plasticity of the photosynthetic apparatus towards altered carotenoid availability (Tardy & Havaux, 1996; Niyogi *et al.*, 1997b; Niyogi *et al.*, 2001), which may be seen as both an evolutionary legacy and wiggle room for future adaptations. Mutants accumulating antheraxanthin instead of violaxanthin have not yet been studied, but could readily be generated by stable transformation of the *aba2* mutant of *N. plumbaginifolia* used here or the ZEP-deficient *npq2* mutants of *A. thaliana* (Niyogi *et al.*, 1998) and *C. reinhardtii* (Niyogi *et al.*, 1997a) with the MeZEP gene.

Experimental Procedures

Plant material and growth conditions

Compsopogon coeruleus (strains SAG 105.79 and SAG 36.94), *C. oishii* (SAG 38.94), *C. hookeri* (SAG 37.94) and *Compsopogonopsis leptoclados* (SAG 106.79) were grown in MiEB12+SWES (10:1) medium at 20 μmol m^{-2} s^{-1} photosynthetically active radiation (PAR), *Erythrotrichia carnea* (SAG 2348) in ½ SWES medium and *Rhodochaete parvula* (SAG 8.99) in SWES medium at 3 μmol m^{-2} s^{-1} PAR. Recipes of culture media are available on the homepage of the Sammlung von Algenkulturen (SAG), Goettingen University, Germany (http://www.uni-goettingen.de/de/list-of-media-and-recipes/186449.html). *Madagascaria erythrocladioides* (CCAP 1342/2) was grown in Modified Provasoli medium according to a recipe of the Culture Collection of Algae and Protozoa (CCAP; https://www.ccap.ac.uk/media/documents/Modified_Provasoli.pdf) at 10 μmol m^{-2} s^{-1} PAR. Algae were grown as 200 ml-batch cultures in 500 ml-Erlenmeyer vessels without shaking at 18 °C with a 16 h light/8 h dark cycle. *Arabidopsis thaliana* (ecotype Col-0) and wild-type and *aba2* mutant of *Nicotiana plumbaginifolia* cv. *viviani* (Marin *et al.*, 1996) were grown in soil pots on irrigation trays containing Hoagland solution at 22 °C and 60 μmol m^{-2} s^{-1} PAR with a 15 h light/9 h dark cycle. The *aba2* plants were grown under clear plastic covers to maintain high humidity, as the ZEP-deficiency makes them prone to wilting.

Identification and in silico analyses of ZEP homologs from red algae

Sequence data from cyanobacteria, glaucophytes, red algae and selected species of other algal groups (see **Tables S1 and S2** for details) available in GenBank (https://www.ncbi.nlm.nih.gov/), the JGI Genome Portal (http://genome.jgi.doe.gov/) and the Microbial Eukaryote Transcriptome Sequencing Project (MMETSP; http://marinemicroeukaryotes.org/project_organisms; Keeling *et al.*, 2014) were searched for ZEP candidates with the BLAST tool (Altschul *et al.*, 1997) using the amino acid sequence of the ZEP from *A. thaliana* (Audran *et al.*, 2001) as input. For mining of MMETSP data, protein and nucleotide assemblies were downloaded from the iMicrobe FTP server (http://ftp.imicrobe.us/) and searched using stand-alone BLAST 2.2.29+ (Camacho *et al.*, 2009). The genome assembly of *P. yezoensis* (Ver. 1; Nakamura *et al.*, 2013) was downloaded from the National Research Institute of Fisheries Science, Japan Fisheries Research and Education Agency (http://nrifs.fra.affrc.go.jp/ResearchCenter/5_BB/genomes/nori/) and the

coding sequence of the ZEP-like protein from *P. yezoensis* (Genbank accession LC026016.1) mapped to the corresponding genomic scaffold using BIOEDIT 5.0.9 (Hall, 1999).

Protein sequences were aligned with CLUSTALW 1.83 (Chenna *et al.*, 2003) and manually refined using BIOEDIT. Maximum likelihood (ML) trees were inferred from the protein alignments using PThreads in RAxML 8.0.14 (Stamatakis, 2014) and the WAG substitution model (Whelan & Goldman, 2001) with gamma rate distribution ('PROTGAMMAWAG', four discrete rate categories). Branch support was estimated with 100 bootstrap replicates using the rapid bootstrap algorithm (Stamatakis *et al.*, 2008) implemented in RAxML PThreads. The phylogenetic tree was visualized using Dendroscope 3.5.8 (Huson & Scornavacca, 2012).

Prediction of N-terminal targeting signals was performed using TargetP 1.1 (Emanuelsson *et al.*, 2007; http://www.cbs.dtu.dk/services/TargetP/), ChloroP 1.1 (Emanuelsson *et al.*, 1999; http://www.cbs.dtu.dk/services/ChloroP/), Predotar 1.04 (Small *et al.*, 2004; https://urgi.versailles.inra.fr/predotar/), iPSORT (Bannai *et al.*, 2002; http://ipsort.hgc.jp/) and PredAlgo (Tardif *et al.*, 2012; https://giavap-genomes.ibpc.fr/cgi-bin/predalgodb.perl?page=main). Cleavage sites of the putative chloroplast transit peptides were predicted by ChloroP 1.1.

Cloning and functional expression of ZEP genes in the tobacco aba2 *mutant*

Genomic DNA and total RNA of *M. erythrocladioides* were each isolated from 100 mg of algal material using the DNeasy® Plant Mini Kit (Qiagen, Hilden, Germany) or the InnuPREP Plant RNA Kit (Analytik Jena, Jena, Germany) according to the manufacturer. cDNA was synthesized from 4 µg of total RNA using the Transcriptor High Fidelity cDNA Synthesis Kit (Roche, Mannheim, Germany) and an anchored-oligo$(dT)_{18}$ primer. For isolation of total RNA of *A. thaliana*, four young leaves were ground in liquid nitrogen, transferred to a 15 ml tube and 2 ml Trizol® (Life Technologies, Darmstadt, Germany) added. Subsequent steps were performed according to Chomczynski & Sacchi (1987). For cDNA synthesis, 5 µg of total RNA were reverse-transcribed using the RevertAid™ H Minus First Strand cDNA Synthesis Kit (Thermo Scientific, Carlsbad, USA) and an oligo$(dT)_{18}$ primer.

PCR reactions were performed with Phusion High-Fidelity DNA Polymerase (Thermo Scientific, Carlsbad, USA). Using the genomic DNA of *M. erythrocladioides* as template, the two alleles of the ZEP gene were amplified using primers MeZEP1-a02p (AGGAAGCCGACAGAATGCTG) and MeZEP1-em

(TTATTAGTTCTGACGGGAGCTCGCCTT) and sequenced on both strands (Starseq, Mainz, Germany) using the PCR primers and primers MeZEP1-s01p (CGAGCAAGCTAGCTCGTATAA), MeZEP1-s02p (CGACGAGCGCGTAGTACTTCTC), MeZEP1-s01m (CTCTCACGCTAGACCAGAT) and MeZEP1-s02m (CCCTCACGCTTGACCAAAT).

Using cDNA as template, the full-length ZEP gene from *A. thaliana* (AtZEP) was amplified using primers AtZEP-s1p (GATCAAGAATTTTAAACGGAG) and AtZEP-e2m (CATGCAAGGAATAGCTGAAA) and ligated into pGEM®-T Easy (Promega, Mannheim, Germany), yielding plasmid pGEM-AtZEP. Using this plasmid as template, the gene fragment encoding the N-teminal transit peptide of AtZEP (tp_{AtZEP} = aa pos. 1-66) was PCR-amplified as two versions with different restriction sites added using AtZEP-ap-NcoI (CCATGGGTTCAACTCCGTTTTG; restriction site in primer sequence underlined) as forward primer and either AtZEP-em-NcoI (CCATGGTCTCAACTAACGCCGTCG, yielding PCR product 1) or AtZEP-em-AvrII-XbaI (TCTAGACTTCAACGCGGCCCTAGGCTCAACTAACGCCGTCG, yielding PCR product 2) as reverse primers. Both PCR products were subcloned into pGEM®-T Easy, then excised and ligated into the pCATgfp vector containing a modified, brightly fluorescent GFP gene under the control of a duplicated cauliflower mosaic virus 35S promoter (Padidam *et al.*, 1999). PCR product 1 was excised with NcoI and ligated into the NcoI site of pCATgfp resulting in a tp_{AtZEP}-GFP-fusion gene (plasmid pCAT-tp_{AtZEP}-GFP). PCR product 2 was excised and ligated into pCATgfp using NcoI and XbaI, leading to replacement of the GFP gene with the tpAtZEP gene fragment (plasmid pCAT-tp_{AtZEP}). For generation of the AtZEP expression construct, the gene fragment encoding the mature AtZEP (aa pos. 67-667) was PCR-amplified from pGEM-AtZEP using primers AtZEP-ap-AvrII (CCTAGGAAGGAGGAGAAGAGAGAGG) and AtZEP-em-PacI-XbaI (TCTAGATTAATTAAGCTTCACCTGAAACCAAG), the product subcloned into pGEM®-T Easy, then excised and ligated into the AvrII and XbaI sites of pCAT-tp_{AtZEP}, yielding plasmid pCAT-AtZEP. Correct orientation and in-frame localization of the inserts was confirmed by sequencing (Starseq, Mainz, Germany). The resulting expression cassettes containing promotor, a gene encoding tpAtZEP fused with either GFP or the mature AtZEP, and a poly-adenylation signal were excised from pCAT using SbfI and ligated into the SbfI site of plasmid pPZP200BAR (Hajdukiewicz *et al.*, 1994; Jozefkowicz *et al.*, 2016), yielding plasmids pPZPbar-tp_{AtZEP}-GFP and pPZPbar-tp_{AtZEP}-AtZEP. Similarly, plasmid pPZPbar-GFP was generated by excision of the cassette containing the GFP gene from pCATgfp with SbfI

and ligation into the SbfI site of pPZP200BAR. The two alleles of the ZEP gene from *M. erythrocladioides* (MeZEP) were amplified from cDNA without the 5'-part encoding the predicted N-terminal presequence by using primers MeZEP1-ap-NcoI (CCTAGGGGACAATCCAGCTGCCCTCGGAGAAG) and MeZEP1-em-PacI (TTAATTAATTATTAGTTCTGACGGGAGCTCGCCTT). The PCR product was subcloned into pGEM®-T Easy and a clone for each allele isolated. The MeZEP alleles were excised with AvrII and PacI and inserted between the AvrII and PacI sites of pPZPbar-tp_{AtZEP}-AtZEP, thereby replacing the gene fragment encoding the mature AtZEP and yielding plasmids pPZPbar-tp_{AtZEP}-MeZEPa1 (allele 1) and pPZPbar-tp_{AtZEP}-MeZEPa2 (allele 2).

For *Agrobacterium*-mediated transformation of the *N. plumbaginifolia aba2* mutant, competent cells of *Agrobacterium tumefaciens* strain LBA4404 were prepared and transformed with the corresponding pPZPbar constructs according to (Höfgen & Willmitzer, 1988). Transformants were grown as 100 ml cultures in YEB medium under selection with 0.6 mM spectinomycin, 0.35 mM streptomycin and 0.06 mM rifampicin at 28 °C and 180 rpm for up to 24 h, the cells harvested by centrifugation (2,000 x g, 5 min, 4 °C), washed in 20 ml infiltration medium (0.5 x MS salts, 10 mM $MgCl_2$, 7.4 mM sucrose, 200 µM acetosyringone, 10 mM MES-KOH, pH 6.1), harvested again by centrifugation, resuspended in infiltration medium to an OD_{600} of ca. 0.6, incubated for 3 h at room temperature and then used for infiltration. Leaves of the upper part of 8-11 weeks old plants were infiltrated from the lower leaf side using a 1 ml-syringe without needle, the suspension being applied comprehensively. Leaves were harvested 4 days after infiltration and leaf disks with a diameter of 7 mm immediately frozen in liquid nitrogen, lyophilized (Alpha 2-4 LD, Christ, Osterode am Harz, Germany) and stored at -20 °C until further analysis. All following analyses were done in triplicate from independent transformants.

Fluorescence microscopy of tobacco leaves transformed with GFP-constructs

Whole leaves were harvested and analyzed 4 days after infiltration using a Leica TCS SP5 II Confocal Microscope and LASAF (Leica application suite) software (Leica, Wetzlar, Germany). Samples were excited by an argon laser (488 nm), GFP fluorescence was detected between 500 and 540 nm and chlorophyll fluorescence between 660 and 720 nm.

Pigment extraction and analysis

General precautions for work with pigments were taken and standard methods for purification of pigments applied (Schiedt & Liaaen Jensen, 1995). For pigment analysis of red algae, thalli from 6-7 week old cultures were dried with paper towel, transferred to 2 ml tubes and methanol equal to 10 times the fresh weight, ethyl acetate equal to 1.3 times the fresh weight and a spatula tip of glass beads (1:3 (w/w) mixture of beads with diameters of 0.25-0.5 mm and 0.75-1 mm) added. For pigment analysis of the lyophilized tobacco leaf discs, 250 µl extraction medium (81.1% methanol (v/v), 10.8% ethyl acetate (v/v), 8.1% water (v/v), 180 mM ammonium acetate) and a spatula tip of glass beads (see above) were added. Samples were homogenized in a Mini-Beadbeater-1 (BioSpec, Bartlesville, USA) at 5,000 rpm for 20 s, cleared by centrifugation (18,400 x g, 3 min) and the supernatant analyzed by HPLC.

HPLC analyses were performed on a Waters Alliance 2795 Separation Module equipped with a Waters 2996 photodiode-array detector; data were collected and analyzed using Waters Empower software (Waters, Eschborn, Germany). Pigments were separated either on HPLC system I described in Blatt *et al.* (2015) or on HPLC system II comprised of an EC 250/4 NUCLEOSIL® 300-5 C18 column equipped with a CC 8/4 NUCLEOSIL® 300-5 C18 guard column (Macherey-Nagel, Düren, Germany) and operated at room temperature (20 °C) by applying a ternary gradient (flow 0.8 ml/min) based on Kraay *et al.* (1992) with linear changes from 60% eluent A (85% methanol buffered with 0.086 M ammonium acetate) and 40% eluent B (90% acetonitrile) at 0 min to 100% eluent B at 2 min, 62% eluent B and 38% eluent C (ethyl acetate) at 13 min, 10% eluent B and 90% eluent C at 14 min, 100% eluent B and 90% eluent C at 17 min, 100% eluent B at 18 min, and 60% eluent A and 40% eluent B at 19 min.

Pigments were identified by comparison of absorbance spectra and retention times with those of reference pigments from a local pigment library (Lohr, 2001). The identity of antheraxanthin from the red algae and the *aba2* mutant of *N. plumbaginifolia* transformed with the ZEP gene from *M. erythrocladioides* was further confirmed by acid-catalyzed furanoid rearrangement of its 5,6-epoxy group (Eugster, 1995) and by *in vitro* de-epoxidation to zeaxanthin using the violaxanthin de-epoxidase from *A. thaliana* (AtVDE). Recombinant AtVDE was prepared by overexpression in *E. coli* Rosetta™ cells using the AtVDE-pET44 plasmid described in Vieler *et al.* (2008). Inclusion bodies containing the AtVDE were purified according to Paulsen *et al.* (1990), the protein denatured and refolded as described in Morosinotto *et al.* (2002) and used for VDE assays according to Goss *et al.* (2005) with

antheraxanthin as substrate and MGDG as only lipid. Lutein epoxide in pigment extracts from tobacco transformants was identified using lutein epoxide isolated from saponified pigment extracts of petals from *Chelidonium majus* (Horvath *et al.*, 2010) as reference and by acid-catalyzed furanoid rearrangement.

Accession Numbers

The MeZEP sequences have been deposited in GenBank under accession numbers MF380407 (genomic allele 1), MF380408 (genomic allele 2), MF152645 (cDNA allele 1) and MF543015 (cDNA allele 2).

Acknowledgements

We thank Annie Marion-Poll (INRA - Centre de Versailles-Grignon, France) for donation of seeds of the *aba2* mutant of *N. plumbaginifolia*, and Kris Niyogi (University of California, Berkeley, USA) for bringing the *Agrobacterium*-mediated transient transformation method to our attention. At Universität Mainz, we are grateful to Wolfgang Wernicke and Marcus Wolf for supplying plasmids pCATgfp and pPZP200BAR, Christoph Rickert for assistance with CLS microscopy, Thomas Igelmund, Christopher Lein, Katharina Mayr, Lisa Mareike Rij and Christine Wendler for technical assistance, and Harald Paulsen for financial support and helpful discussions. The authors declare no conflict of interest.

Author Contribution

M.L. planned and designed the research, M.L. and O.D. designed experiments, O.D. performed experiments, O.D. and M.L. analysed the data, and M.L. wrote the manuscript with input from O.D.. This work represents part of O.D.'s PhD dissertation.

Short Supporting Information Legends

The following Supporting Information is available for this article:

Table S1. Database accessions of ZEP sequences from algae and land plants included in the phylogenetic tree in Figure 2a.

Table S2. Database accessions of cyanobacterial sequences annotated as ZEP in GenBank and included in the phylogenetic tree in Figure 2a.

Data S1. Sequence assembly of the ZEP gene from *Compsopogon coeruleus*.

Data S2. Sequence assembly of the ZEP gene from *Madagascaria erythrocladioides*.

Data S3. Sequence assembly of the ZEP gene from *Calliarthron tuberculosum*.

Data S4. Sequence assembly of the ZEP-like gene from *Porphyra purpurea*.

Data S5. Sequence assembly of the ZEP-like gene from *Porphyra umbilicalis*.

Data S6. Mapping of the ZEP-like gene from *Pyropia yezoensis* to the corresponding genomic scaffold in search for alternative start codons.

Data S7. Extension of N-termini of the ZEP-like proteins from *Porphyra purpurea*, *P. umbilicalis* and *Pyropia yezoensis* does not identify alternative start codons.

References

Aihara, M.S. and Yamamoto, H.Y. (1968) Occurrence of antheraxanthin in two Rhodophyceae *Acanthophora spicifera* and *Gracilaria lichenoides*. *Phytochemistry* **7**, 497-499.

Altschul, S.F., Madden, T.L., Schaffer, A.A., Zhang, J.H., Zhang, Z., Miller, W. and Lipman, D.J. (1997) Gapped BLAST and PSI-BLAST: a new generation of protein database search programs. *Nucleic Acids Res.* **25**, 3389-3402.

Andersson, M., Schubert, H., Pedersen, M. and Snoeijs, P. (2006) Different patterns of carotenoid composition and photosynthesis acclimation in two tropical red algae. *Mar. Biol.* **149**, 653-665.

Audran, C., Liotenberg, S., Gonneau, M., North, H., Frey, A., Tap-Waksman, K., Vartanian, N. and Marion-Poll, A. (2001) Localisation and expression of zeaxanthin epoxidase mRNA in Arabidopsis in response to drought stress and during seed development. *Aust. J. Plant Physiol.* **28**, 1161-1173.

Bannai, H., Tamada, Y., Maruyama, O., Nakai, K. and Miyano, S. (2002) Extensive feature detection of N-terminal protein sorting signals. *Bioinformatics* **18**, 298-305.

Baroli, I., Do, A.D., Yamane, T. and Niyogi, K.K. (2003) Zeaxanthin accumulation in the absence of a functional xanthophyll cycle protects *Chlamydomonas reinhardtii* from photooxidative stress. *Plant Cell* **15**, 992-1008.

Bjørnland, T., Borch, G. and Liaaen-Jensen, S. (1984) Configurational studies on red algae carotenoids. *Phytochemistry* **23** 1711-1716.

Blatt, A., Bauch, M.E., Pörschke, Y. and Lohr, M. (2015) A lycopene β-cyclase/lycopene ε-cyclase/light-harvesting complex-fusion protein from the green alga *Ostreococcus*

lucimarinus can be modified to produce α-carotene and β-carotene at different ratios. *Plant J*. **82**, 582-595.

Brown, L.M. and Mclachlan, J. (1982) Atypical carotenoids for the Rhodophyceae in the genus Gracilaria (Gigartinales). *Phycologia* **21**, 9-16.

Büch, K., Stransky, H. and Hager, A. (1995) FAD Is a further essential cofactor of the NAD(P)H and O_2-dependent zeaxanthin-epoxidase. *FEBS Lett*. **376**, 45-48.

Camacho, C., Coulouris, G., Avagyan, V., Ma, N., Papadopoulos, J., Bealer, K. and Madden, T.L. (2009) BLAST+: architecture and applications. *BMC Bioinformatics* **10**, 421.

Cavalier-Smith, T., Chao, E.E. and Lewis, R. (2015) Multiple origins of Heliozoa from flagellate ancestors: New cryptist subphylum Corbihelia, superclass Corbistoma, and monophyly of Haptista, Cryptista, Hacrobia and Chromista. *Mol. Phylogenet. Evol.* **93**, 331-362.

Chenna, R., Sugawara, H., Koike, T., Lopez, R., Gibson, T.J., Higgins, D.G. and Thompson, J.D. (2003) Multiple sequence alignment with the Clustal series of programs. *Nucleic Acids Res.* **31**, 3497-3500.

Chomczynski, P. and Sacchi, N. (1987) Single-step method of RNA isolation by acid guanidinium thiocyanate-phenol-chloroform extraction. *Anal. Biochem*. **162**, 156-159.

Coesel, S., Oborník, M., Varela, J., Falciatore, A. and Bowler, C. (2008) Evolutionary origins and functions of the carotenoid biosynthetic pathway in marine diatoms. *PLoS ONE* **3**, e2896.

Eilers, U., Dietzel, L., Breitenbach, J., Buchel, C. and Sandmann, G. (2016) Identification of genes coding for functional zeaxanthin epoxidases in the diatom *Phaeodactylum tricornutum*. *J. Plant Physiol.* **192**, 64-70.

Emanuelsson, O., Brunak, S., von Heijne, G. and Nielsen, H. (2007) Locating proteins in the cell using TargetP, SignalP and related tools. *Nat. Protoc*. **2**, 953-971.

Emanuelsson, O., Nielsen, H. and Von Heijne, G. (1999) ChloroP, a neural network-based method for predicting chloroplast transit peptides and their cleavage sites. *Protein Sci.* **8**, 978-984.

Esteban, R., Martínez, B., Fernández-Marín, B., Becerril, J.M. and García-Plazaola, J.I. (2009) Carotenoid composition in Rhodophyta: insights into xanthophyll regulation in *Corallina elongata*. *Eur. J. Phycol.* **44**, 221-230.

Eugster, C.H. (1995) Chemical derivatization: Microscale tests for the presence of common functional groups in carotenoids. In *Carotenoids, Vol. 1A, Isolation and Analysis* (Britton, G., Liaaen-Jensen, S. and Pfander, H. eds). Basel, Boston, Berlin: Birkhäuser, pp. 71-80.

Frommolt, R., Werner, S., Paulsen, H., Goss, R., Wilhelm, C., Zauner, S., Maier, U.G., Grossman, A.R., Bhattacharya, D. and Lohr, M. (2008) Ancient recruitment by chromists of green algal genes encoding enzymes for carotenoid biosynthesis. *Mol. Biol. Evol.* **25**, 2653-2667.

Gantt, E., Berg, G.M., Bhattacharya, D., Blouin, N.A., Brodie, J., Chan, C.X., Collén, J., Cunningham, F.X., Gross, J., Grossman, A.R., Karpowicz, S., Kitade, Y., Klein, A.S., Levine, I.A., Lin, S., Lu, S., Lynch, M., Minocha, S.C., Müller, K.M., Neefus, C.D., Oliveira, M.C., Rymarquis, L., Smith, A., Stiller, J.W., Wu, W.-K., Yarish, C., Zhuang, Y.Y. and Brawley, S.H. (2010) *Porphyra*: complex life histories in a harsh environment. *P. umbilicalis*, an intertidal red alga for genomic analysis. In *Red Algae in the Genomic Age* (Seckbach, J. and Chapman, D.J. eds). Dordrecht, Heidelberg, London, New York: Springer, pp. 129-148.

Goodwin, T.W. (1980) *The Biochemistry of the Carotenoids, Vol. I: Plants; 2nd ed.* London, New York: Chapman & Hall.

Goss, R. and Lepetit, B. (2015) Biodiversity of NPQ. *J. Plant. Physiol.* **172**, 13-32.

Goss, R., Lohr, M., Latowski, D., Grzyb, J., Vieler, A., Wilhelm, C. and Strzalka, K. (2005) Role of hexagonal structure-forming lipids in diadinoxanthin and violaxanthin solubilization and de-epoxidation. *Biochemistry* **44**, 4028-4036.

Gould, S.B., Maier, U.G. and Martin, W.F. (2015) Protein import and the origin of red complex plastids. *Curr. Biol*. **25**, R515-R521.

Hajdukiewicz, P., Svab, Z. and Maliga, P. (1994) The small, versatile *pPZP* family of *Agrobacterium* binary vectors for plant transformation. *Plant Mol Biol.* **25**, 989-994.

Hall, T.A. (1999) BioEdit: a user-friendly biological sequence alignment editor and analysis program for Windows 95/98/NT. *Nucleic Acids Symp. Ser.* **41**, 95-98.

Höfgen, R. and Willmitzer, L. (1988) Storage of competent cells for Agrobacterium transformation. *Nucleic Acids Res.* **16**, 9877-9877.

Horvath, G., Molnar, P., Farkas, A., Szabo, L.G., Turcsi, E. and Deli, J. (2010) Separation and identification of carotenoids in flowers of *Chelidonium majus* L. and inflorescences of *Solidago canadensis* L. *Chromatographia* **71**, S103-S108.

Huson, D.H. and Scornavacca, C. (2012) Dendroscope 3: An interactive tool for rooted phylogenetic trees and networks. *Syst. Biol*. **61**, 1061-1067.

Jackson, C.J. and Reyes-Prieto, A. (2014) The mitochondrial genomes of the glaucophytes *Gloeochaete wittrockiana* and *Cyanoptyche gloeocystis*: Multilocus phylogenetics suggests a monophyletic Archaeplastida. *Genome Biol. Evol.* **6**, 2774-2785.

Jeffrey, S.W., Wright, S.W. and Zapata, M. (2011) Micoralgal classes and their signature pigments. In *Phytoplankton Pigments. Characterization, Chemotaxonomy and Applications in Oceanography* (Roy, S., Llewellyn, C.A., Egeland, E.S. and Johnsen, G. eds). Cambridge: Cambridge University Press, pp. 3-77.

Jozefkowicz, C., Bottero, E., Pascuan, C., Pagano, E., Ayub, N.D. and Soto, G. (2016) Minimizing the time and cost of production of transgenic alfalfa libraries using the highly efficient completely sequenced vector pPZP200BAR. *Plant Cell Rep.* **35**, 1987-1990.

Keeling, P.J., Burki, F., Wilcox, H.M., Allam, B., Allen, E.E., Amaral-Zettler, L.A., Armbrust, E.V., Archibald, J.M., Bharti, A.K., Bell, C.J., Beszteri, B., Bidle, K.D., Cameron, C.T., Campbell, L., Caron, D.A., Cattolico, R.A., Collier, J.L., Coyne, K., Davy, S.K., Deschamps, P., Dyhrman, S.T., Edvardsen, B., Gates, R.D., Gobler, C.J., Greenwood, S.J., Guida, S.M., Jacobi, J.L., Jakobsen, K.S., James, E.R., Jenkins, B., John, U., Johnson, M.D., Juhl, A.R., Kamp, A., Katz, L.A., Kiene, R., Kudryavtsev, A., Leander, B.S., Lin, S., Lovejoy, C., Lynn, D., Marchetti, A., McManus, G., Nedelcu, A.M., Menden-Deuer, S., Miceli, C., Mock, T., Montresor, M., Moran, M.A., Murray, S., Nadathur, G., Nagai, S., Ngam, P.B., Palenik, B., Pawlowski, J., Petroni, G., Piganeau, G., Posewitz, M.C., Rengefors, K., Romano, G., Rumpho, M.E., Rynearson, T., Schilling, K.B., Schroeder, D.C., Simpson, A.G.B., Slamovits, C.H., Smith, D.R., Smith, G.J., Smith, S.R., Sosik, H.M., Stief, P., Theriot, E., Twary, S., Umale, P.E., Vaulot, D., Wawrik, B., Wheeler, G.L., Wilson, W.H., Xu, Y., Zingone, A. and Worden, A.Z. (2014) The Marine Microbial Eukaryote Transcriptome Sequencing Project (MMETSP): Illuminating the functional diversity of eukaryotic life in the oceans through transcriptome sequencing. *PLoS Biol* **12**, e1001889.

Kosourov, S., Murukesan, G., Jokela, J. and Allahverdiyeva, Y. (2016) Carotenoid biosynthesis in *Calothrix* sp. 336/3: Composition of carotenoids on full medium, during diazotrophic growth and after long-term H_2 photoproduction. *Plant Cell Physiol.* **57**, 2269-2282.

Kraay, G.W., Zapata, M. and Veldhuis, M.J.W. (1992) Separation of chlorophylls c_1, c_2, and c_3 of marine phytoplankton by reversed-phase-C_{18}-high-performance liquid chromatography. *J. Phycol.* **28**, 708-712.

Leonelli, L., Erickson, E., Lyska, D. and Niyogi, K.K. (2016) Transient expression in *Nicotiana benthamiana* for rapid functional analysis of genes involved in non-photochemical quenching and carotenoid biosynthesis. *Plant J.* **88**, 375-386.

Li, B., Lopes, J.S., Foster, P.G., Embley, T.M. and Cox, C.J. (2014) Compositional biases among synonymous substitutions cause conflict between gene and protein trees for plastid origins. *Mol. Biol. Evol.* **31**, 1697-1709.

Lohr, M. (2001) *Beziehungen zwischen den Xanthophyllzyklen und der Biosynthese von Lichtsammelxanthophyllen in Chlorophyll a/c-haltigen Algen*. Ph.D. thesis, Johannes Gutenberg-Universität Mainz, Germany.

Lohr, M. and Wilhelm, C. (1999) Algae displaying the diadinoxanthin cycle also possess the violaxanthin cycle. *Proc. Natl. Acad. Sci. U. S. A.* **96**, 8784-8789.

Lohr, M. and Wilhelm, C. (2001) Xanthophyll synthesis in diatoms: quantification of putative intermediates and comparison of pigment conversion kinetics with rate constants derived from a model. *Planta* **212**, 382-391.

Lokstein, H., Tian, L., Polle, J.E.W. and DellaPenna, D. (2002) Xanthophyll biosynthetic mutants of Arabidopsis thaliana: altered nonphotochemical quenching of chlorophyll fluorescence is due to changes in Photosystem II antenna size and stability. *Biochim. Biophys. Acta - Bioenerg.* **1553**, 309-319.

Marin, E., Nussaume, L., Quesada, A., Gonneau, M., Sotta, B., Hugueney, P., Frey, A. and Marion-Poll, A. (1996) Molecular identification of zeaxanthin epoxidase of *Nicotiana plumbaginifolia*, a gene involved in abscisic acid biosynthesis and corresponding to the ABA locus of *Arabidopsis thaliana*. *EMBO J.* **15**, 2331-2342.

Marquardt, J. and Hanelt, D. (2004) Carotenoid composition of *Delesseria lancifolia* and other marine red algae from polar and temperate habitats. *Eur. J. Phycol.* **39**, 285-292.

Mikami, K., Mori, I.C., Matsuura, T., Ikeda, Y., Kojima, M., Sakakibara, H. and Hirayama, T. (2016) Comprehensive quantification and genome survey reveal the presence of novel phytohormone action modes in red seaweeds. *J. Appl. Phycol.* **28**, 2539-2548.

Morosinotto, T., Baronio, R. and Bassi, R. (2002) Dynamics of chromophore binding to Lhc proteins *in vivo* and *in vitro* during operation of the xanthophyll cycle. *J. Biol. Chem.* **277**, 36913-36920.

Moustafa, A., Beszteri, B., Maier, U.G., Bowler, C., Valentin, K. and Bhattacharya, D. (2009) Genomic footprints of a cryptic plastid endosymbiosis in diatoms. *Science* **324**, 1724-1726.

Nakamura, Y., Sasaki, N., Kobayashi, M., Ojima, N., Yasuike, M., Shigenobu, Y., Satomi, M., Fukuma, Y., Shiwaku, K., Tsujimoto, A., Kobayashi, T., Nakayama, I., Ito, F., Nakajima, K., Sano, M., Wada, T., Kuhara, S., Inouye, K., Gojobori, T. and Ikeo, K. (2013). The first symbiont-free genome sequence of marine red alga, Susabi-nori (*Pyropia yezoensis*). *PLoS ONE* **8**, e57122.

Nambara, E. and Marion-Poll, A. (2005) Abscisic acid biosynthesis and catabolism. *Annu. Rev. Plant Biol.* **56**, 165-185.

Niyogi, K.K., Björkman, O. and Grossman, A.R. (1997a) *Chlamydomonas* xanthophyll cycle mutants identified by video imaging of chlorophyll fluorescence quenching. *Plant Cell* **9**, 1369-1380.

Niyogi, K.K., Björkman, O. and Grossman, A.R. (1997b) The roles of specific xanthophylls in photoprotection. *Proc. Natl. Acad. Sci. U. S. A.* **94**, 14162-14167.

Niyogi, K.K., Grossman, A.R. and Björkman, O. (1998) *Arabidopsis* mutants define a central role for the xanthophyll cycle in the regulation of photosynthetic energy conversion. *Plant Cell* **10**, 1121-1134.

Niyogi, K.K., Shih, C., Chow, W.S., Pogson, B.J., DellaPenna, D. and Björkman, O. (2001) Photoprotection in a zeaxanthin- and lutein-deficient double mutant of *Arabidopsis*. *Photosynth. Res.* **67**, 139-145.

Padidam, M., Reddy, V.S., Beachy, R.N. and Fauquet, C.M. (1999) Molecular characterization of a plant mitochondrial chaperone GrpE. *Plant Mol. Biol.* **39**, 871-881.

Patron, N.J. and Waller, R.F. (2007) Transit peptide diversity and divergence: a global analysis of plastid targeting signals. *Bioessays* **29**, 1048-1058.

Paulsen, H., Rümler, U. and Rüdiger, W. (1990) Reconstitution of pigment-containing complexes from light-harvesting chlorophyll-a/b-binding protein overexpressed in *Escherichia coli*. *Planta* **181**, 204-211.

Pogson, B., McDonald, K.A., Truong, M., Britton, G. and DellaPenna, D. (1996) *Arabidopsis* carotenoid mutants demonstrate that lutein is not essential for photosynthesis in higher plants. *Plant Cell* **8**, 1627-1639.

Pogson, B.J., Niyogi, K.K., Björkman, O. and DellaPenna, D. (1998) Altered xanthophyll compositions adversely affect chlorophyll accumulation and nonphotochemical quenching in *Arabidopsis* mutants. *Proc. Natl. Acad. Sci. U. S. A.* **95**, 13324-13329.

Price, D.C., Chan, C.X., Yoon, H.S., Yang, E.C., Qiu, H., Weber, A.P.M., Schwacke, R., Gross, J., Blouin, N.A., Lane, C., Reyes-Prieto, A., Durnford, D.G., Neilson, J.A.D., Lang, B.F., Burger, G., Steiner, J.M., Loffelhardt, W., Meuser, J.E., Posewitz, M.C., Ball, S., Arias, M.C., Henrissat, B., Coutinho, P.M., Rensing, S.A., Symeonidi, A., Doddapaneni, H., Green, B.R.,

Rajah, V.D., Boore, J. and Bhattacharya, D. (2012) *Cyanophora paradoxa* genome elucidates origin of photosynthesis in algae and plants. *Science* **335**, 843-847.

Ruban, A.V. (2016) Nonphotochemical chlorophyll fluorescence quenching: mechanism and effectiveness in protecting plants from photodamage. *Plant Physiol.* **170**, 1903-1916.

Schiedt, K. and Liaaen Jensen, S. (1995) Isolation and analysis. In *Carotenoids, Vol. 1A, Isolation and Analysis* (Britton, G., Liaaen-Jensen, S. and Pfander, H. eds). Basel, Boston, Berlin: Birkhäuser, pp. 81-108.

Schubert, N. and García-Mendoza, E. (2008) Photoinhibition in red algal species with different carotenoid profiles. *J. Phycol.* **44**, 1437-1446.

Schubert, N., García-Mendoza, E. and Pacheco-Ruiz, I. (2006) Carotenoid composition of marine red algae. *J. Phycol.* **42**, 1208-1216.

Schwarz, N., Armbruster, U., Iven, T., Bruckle, L., Melzer, M., Feussner, I. and Jahns, P. (2015) Tissue-specific accumulation and regulation of zeaxanthin epoxidase in Arabidopsis reflect the multiple functions of the enzyme in plastids. *Plant Cell Physiol*. **56**, 346-357.

Siefermann, D. and Yamamoto, H.Y. (1975) Properties of NADP and oxygen-dependent zeaxanthin epoxidation in isolated chloroplasts - a transmembrane model for the violaxanthin cycle. *Arch. Biochem. Biophys.* **171**, 70-77.

Small, I., Peeters, N., Legeai, F. and Lurin, C. (2004) Predotar: A tool for rapidly screening proteomes for N-terminal targeting sequences. *Proteomics* **4**, 1581-1590.

Stamatakis, A. (2014) RAxML version 8: a tool for phylogenetic analysis and post-analysis of large phylogenies. *Bioinformatics* **30**, 1312-1313.

Stamatakis, A., Hoover, P. and Rougemont, J. (2008) A Rapid Bootstrap Algorithm for the RAxML Web Servers. *Syst. Biol.* **57**, 758-771.

Steiner, J.M. and Löffelhardt, W. (2005) Protein translocation into and within cyanelles (Review). *Mol. Membr. Biol.* **22**, 123-132.

Stiller, J.W., Schreiber, J., Yue, J.P., Guo, H., Ding, Q. and Huang, J.L. (2014) The evolution of photosynthesis in chromist algae through serial endosymbioses. *Nat. Commun*. **5**, 5764, doi:5710.1038/ncomms6764.

Swift, I.E. and Milborrow, B.V. (1981) Stereochemistry of allene biosynthesis and the formation of the acetylenic carotenoid diadinoxanthin and peridinin (C_{37}) from neoxanthin. *Biochem. J.* **199**, 69-74.

Takaichi, S. and Mochimaru, M. (2007) Carotenoids and carotenogenesis in cyanobacteria: unique ketocarotenoids and carotenoid glycosides. *Cell. Mol. Life Sci.* **64**, 2607-2619.

Takaichi, S., Yokoyama, A., Mochimaru, M., Uchida, H. and Murakami, A. (2016) Carotenogenesis diversification in phylogenetic lineages of Rhodophyta. *J. Phycol.* **52**, 329-338.

Tardif, M., Atteia, A., Specht, M., Cogne, G., Rolland, N., Brugiere, S., Hippler, M., Ferro, M., Bruley, C., Peltier, G., Vallon, O. and Cournac, L. (2012) PredAlgo: A new subcellular localization prediction tool dedicated to green algae. *Mol. Biol. Evol.* **29**, 3625-3639.

Tardy, F. and Havaux, M. (1996) Photosynthesis, chlorophyll fluorescence, light-harvesting system and photoinhibition resistance of a zeaxanthin-accumulating mutant of *Arabidopsis thaliana*. *J. Photochem. Photobiol. B - Biol.* **34**, 87-94.

van Berkel, W.J.H., Kamerbeek, N.M. and Fraaije, M.W. (2006) Flavoprotein monooxygenases, a diverse class of oxidative biocatalysts. *J. Biotechnol.* **124**, 670-689.

Vieler, A., Scheidt, H.A., Schmidt, P., Montag, C., Nowoisky, J.F., Lohr, M., Wilhelm, C., Huster, D. and Goss, R. (2008) The influence of phase transitions in phosphatidylethanolamine models on the activity of violaxanthin de-epoxidase. *Biochim. Biophys. Acta - Biomembranes* **1778**, 1027-1034.

Whelan, S. and Goldman, N. (2001) A general empirical model of protein evolution derived from multiple protein families using a maximum-likelihood approach. *Mol. Biol. Evol.* **18**, 691-699.

Yamamoto, H.Y. and Higashi, R.M. (1978) Violaxanthin de-epoxidase. Lipid composition and substrate specificity. *Arch. Biochem. Biophys.* **190**, 514-522.

Yang, E.C., Boo, S.M., Bhattacharya, D., Saunders, G.W., Knoll, A.H., Fredericq, S., Graf, L. and Yoon, H.S. (2016) Divergence time estimates and the evolution of major lineages in the florideophyte red algae. *Sci. Rep.* **6**, 21361.

Yang, L.E., Huang, X.Q., Hang, Y., Deng, Y.Y., Lu, Q.Q. and Lu, S. (2014) The P450-type carotene hydroxylase PuCHY1 from *Porphyra* suggests the evolution of carotenoid metabolism in red algae. *J. Integr. Plant Biol.* **56**, 902-915.

Yoon, H.S., Hackett, J.D., Ciniglia, C., Pinto, G. and Bhattacharya, D. (2004) A molecular timeline for the origin of photosynthetic eukaryotes. *Mol. Biol. Evol.* **21**, 809-818.

Yoon, H.S., Muller, K.M., Sheath, R.G., Ott, F.D. and Bhattacharya, D. (2006) Defining the major lineages of red algae (Rhodophyta). *J. Phycol.* **42**, 482-492.

Table 1. Rhodophyta reported to contain the epoxy-carotenoids antheraxanthin (Ant) and violaxanthin (Vio). For species resp. strains in bold and underlined, zeaxanthin epoxidase (ZEP) genes have been identified in this study. Concentrations of epoxy-carotenoids are expressed as % of total carotenoids. Only algae with antheraxanthin content reported to exceed 10 % of total carotenoids have been included.

Taxa (Strain)	% Ant	% Vio	Reference
Compsopogonophyceae			
Compsopogonales			
Compsopogon coeruleus (natural sample)	31		Takaichi et al., 2016
***C. coeruleus* (SAG 36.94)**	56	-	This study
C. coeruleus (SAG 105.79)	62	-	This study
C. hookeri (SAG 37.94)	56	-	This study
C. oishii (SAG 38.94)	54	-	This study
Compsopogonopsis leptoclados (SAG 106.7)	55	-	This study
Erythropeltidales			
Erythrotrichia carnea (unialgal culture)	65		Bjørnland, 1984
E. carnea (SAG 2348)	65	<1	This study
***Madagascaria erythrocladioides* (CCAP 1342/2)**	64	-	This study
Rhodochaete parvula (SAG 8.33)	47	<1	This study
Sahlingia subintegra (AYCC185)	65		Takaichi et al., 2016
Smithora naiadum (natural sample)	34	2	Schubert et al., 2006
Florideophyceae			
Corallinales			
Bossiella californica (natural sample)	70	5	Schubert et al., 2006
B. orbignyana (natural sample)	61	2	Schubert et al., 2006
Calliarthron cheilosporioides (natural sample)	82		Schubert & Garcia-Mendoza, 2008
C. tuberculosum (natural sample)	78	1	Schubert et al., 2006
Corallina elongata (natural sample)	41		Esteban et al., 2009
C. officinalis (natural sample)	57	3	Schubert et al., 2006
C. pilulifera (natural sample)	40		Takaichi et al., 2016
C. vancouverensis (natural sample)	67	1	Schubert et al., 2006
Jania rubens (natural sample)	38		Esteban et al., 2009
J. tenella (natural sample)	69	4	Schubert et al., 2006
Ceramiales			

Acanthophora spicifera (natural sample)	32		Aihara & Yamamoto, 1968
Delesseria lancifolia (AWI 2131)	49	20	Marquardt & Hanelt, 2004
Gracilariales			
Gracilaria birdiae (unialgal culture)	45	3	Ursi et al., 2006
G. bursapastoris (NRCC S-130)	41	8	Brown & McLachlan, 1982
G. coronopifolia (NRCC S-68)	45	3	Brown & McLachlan, 1982
G. domingensis (unialgal culture)	60	1	Andersson et al., 2006
G. foliifera (NRCC S-39)	48	4	Brown & McLachlan, 1982
G. lichenoides (natural sample)	25		Aihara & Yamamoto, 1968
G. salicornia (NRCC S-66)	51	4	Brown & McLachlan, 1982
G. textorii (natural sample)	32	2	Schubert et al., 2006
G. tikvahiae (NRCC WT-138)	50	2	Brown & McLachlan, 1982
G. turgida (NRCC S-73)	46	5	Brown & McLachlan, 1982
G. verrucosa (NRCC S-80x)	34	14	Brown & McLachlan, 1982
Gracilariopsis lemaneiformis (natural sample)	19	1	Schubert et al., 2006

Figure Legends

Figure 1. Occurrence and biosynthetic relation of carotenoids with epoxy, allenic and acetylenic groups in photosynthetic eukaryotes. Filled circles indicate general occurrence in Glaucophyta (blue), Rhodophyta (red), Viridiplantae (green) or Chromalveolata (orange), while sectors indicate that the carotenoid is not present in all species of the respective taxon. With the exception of diatoxanthin, all allenic and acetylenic carotenoids mentioned contain an epoxy group at the other end of the molecule. Steps catalyzed by zeaxanthin epoxidases are labeled with ZEP; red dotted arrows indicate de-epoxidation steps catalyzed by violaxanthin de-epoxidase under light stress.

Figure 2. *In silico* analyses of zeaxanthin epoxidase (ZEP) candidates from red algae and cyanobacteria. (a) Phylogenetic affiliation of candidate ZEP proteins from red algae with ZEP proteins from Viridiplantae and Chromalveolata and with cyanobacterial proteins annotated as ZEP proteins in the GenBank database solely based on sequence similarity. The midpoint-rooted ML tree (RAxML) was constructed from a protein alignment with 458 distinct alignment patterns. Filled circles label major nodes with bootstrap support (100 replicates) higher than 90% and open circles major nodes with support higher than 80 %. Source names of ZEP proteins with experimentally confirmed catalytic function are underlined and labeled with asterisks. (b) Alignment of the N-termini and targeting prediction of the candidate ZEP

proteins from *Calliarthron tuberculosum* and *Madagascaria erythrocladioides*, the ZEP-like proteins from three Bangiales (species names in red) and cyanobacterial proteins (species names in blue) annotated as ZEP proteins in GenBank. Conserved sites in the alignment are indicated by black boxes for identical and gray boxes for similar amino acids. Prediction of transit peptides for import into plastids (C) or mitochondria (M) and of signal peptides (S) was done using TargetP (TrP), PredAlgo (PrA), Predotar (Prd), iPSORT (iPS) and ChloroP (ChP). Chloroplast transit peptides predicted by ChloroP are underlined and diagnostic phenylalanine residues labeled in red. For TargetP results, reliability classes (1-5) are given in brackets, with lower values indicating more reliable predictions. See **Tables S1 and S2** for full species names and sequence accessions.

Figure 3. Identification of antheraxanthin in the red alga *Madagascaria erythrocladioides*. (a) Analysis of a pigment extract from *M. erythrocladioides* using HPLC system I identified antheraxanthin (peak 4), zeaxanthin (7), chlorophyll a (8) and β-carotene (9). The identification of peak 4 as antheraxanthin was confirmed by (b) acid-catalyzed furanoid rearrangement leading to a hypsochromic shift of the absorbance spectrum by about 20 nm and (c) *in vitro* de-epoxidation to zeaxanthin (7) by violaxanthin de-epoxidase (VDE) from *Arabidopsis thaliana* using HPLC system II for pigment analysis.

Figure 4. *Agrobacterium*-mediated functional expression of zeaxanthin epoxidase (ZEP) enzymes in the ZEP-deficient *aba2* mutant of *Nicotiana plumbaginifolia*. (a) Activity of the ZEP expression products detected by comparative analyses (HPLC system I) of pigment extracts from leafs of an untreated *aba2* mutant, a wild-type plant, the *aba2* mutant transiently transformed with the ZEP from *Arabidopsis thaliana* (tp_{AtZEP}-AtZEP), and the *aba2* mutant transiently transformed with the ZEP candidate from *Madagascaria erythrocladioides* fused to the transit peptide of the ZEP from *A. thaliana* (tp_{AtZEP}-MeZEP; result shown for allele 1). Leaves transformed with the empty vector had the same pigment pattern as untreated leaves. Peaks represent violaxanthin (1), 9'-*cis*-neoxanthin (2), lutein epoxide (3), antheraxanthin (4), lutein (5), chlorophyll b (6), zeaxanthin (7), chlorophyll a (8) and β-carotene (9). The transit peptide from the ZEP of *A. thaliana* also mediated plastid import of GFP as demonstrated by confocal laser scanning microscopy (b-g). Microscopic sections of leaves from *aba2* mutants transformed with either tp_{AtZEP}-GFP (b-d) or GFP (e-g) showing transmission images (b, e), chlorophyll fluorescence of plastids (c, f) and localization of GFP fluorescence (d, g) in the corresponding mesophyll cells. All analyses were done in triplicate from independent transformants, with the figure showing representative results.

Figure 1

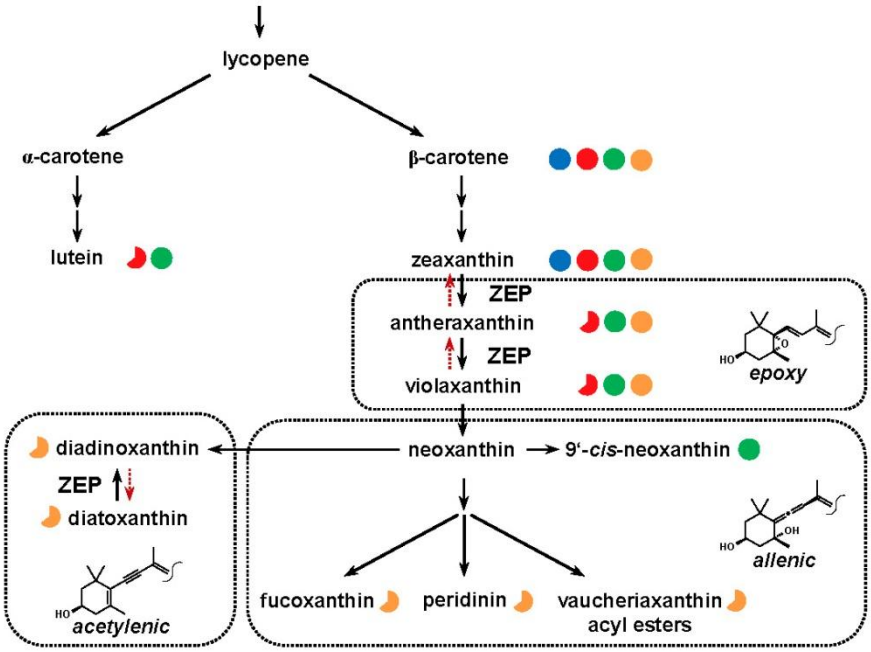

Figure 2

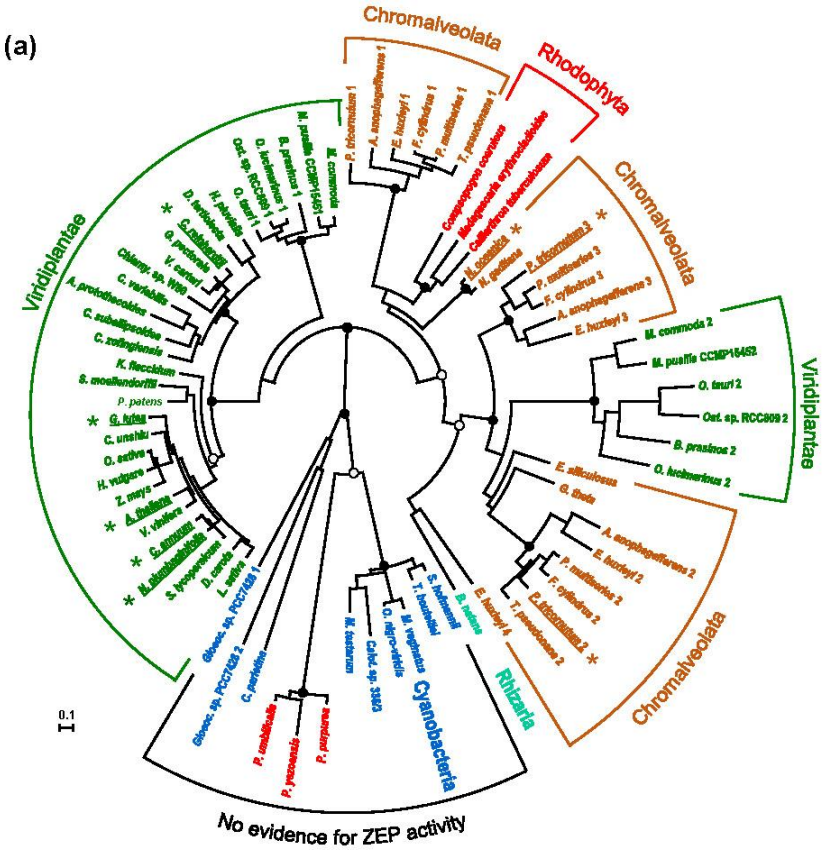

Figure 3

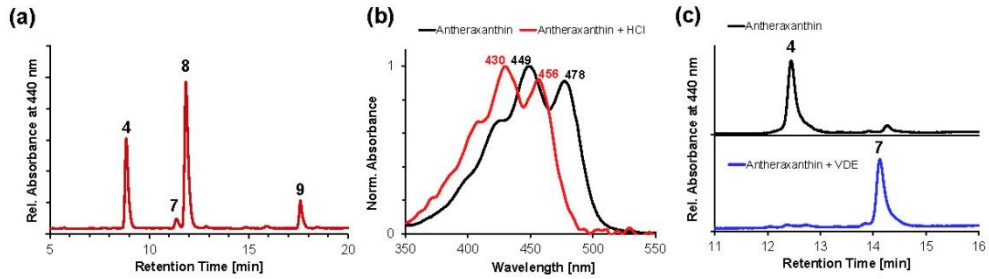

Figure 4